Spectroscopic Studies of Fullerene Aggregates

T. Rudalevige and A. H. Francis*

Department of Chemistry, The University of Michigan, Ann Arbor, Michigan 48109

R. Zand

Department of Biological Chemistry and the Biophysical Research Division, The University of Michigan, Ann Arbor, Michigan 48109

Received: August 4, 1998; In Final Form: October 6, 1998

The growth and structure of fullerene (C_{60} and C_{70}) aggregates in single and binary mixed-solvent solutions were examined by light scattering and photoluminescence spectroscopy. Solute aggregation exhibiting reaction-limited kinetics was observed to occur over a period of several days in ~1 mM C_{60} solutions in benzene. Aggregation was irreversible and could be suppressed by addition of a soluble radical scavenger, suggesting a radical mechanism for aggregate formation. Dynamic light scattering measurements determined that the aggregates attain a hydrodynamic radius of ~300 nm before sedimentation occurs. Solutions containing stable suspensions of fullerene aggregates were also prepared by addition of a poor solvent to a solution of fullerene in a strong solvent. Both static and dynamic light scattering methods were used to determine the mass, hydrodynamic radius, radius of gyration, and fractal dimension of the aggregates. Photoluminescence spectra of aggregates were compared with those of the crystalline materials. The luminescence spectra of solutions containing aggregates were found to differ substantially from the luminescence spectra of unassociated fullerene. The chief effect of aggregate formation is the appearance of excimer-like features in the photoluminescence spectrum.

Introduction

In studies of the electronic spectra of C_{60} and C_{70}, numerous investigators have noted extreme solvatochromism and other environmental effects.[1] These arise in part because the fullerenes are good electrophiles and may form both ground and excited-state complexes with π-electron-donating aromatic solvents.[2] Since transitions to the lower excited states are forbidden by strong selection rules based on the high molecular symmetry, the symmetry-breaking effects arising from environmental interactions may have dramatic spectroscopic consequences. To analyze the spectra of fullerenes, it is necessary to distinguish intramolecular effects (e.g., Jahn−Teller distortions, Herzberg−Teller vibronic coupling) from intermolecular effects (e.g., solvatochromism, solute aggregation, complex formation). In the present work, we focus on the phenomenon of fullerene aggregate formation in solution and its effect on the electronic spectra of C_{60} and C_{70}.

Most studies of fullerene aggregation have focused on the behavior of C_{60}. The earliest evidence of fullerene aggregate formation in solution was provided by studies of the temperature dependence of the solubility of C_{60}. Ruoff et al.[3] discovered that the solubility of C_{60} in benzene, instead of increasing with temperature, peaked at ~280 K and then decreased over a narrow temperature range. Bezmelnitsin et al.[4] proposed that this behavior resulted from the formation of solute aggregates and proposed that dissolution of the aggregates above 280 K increases the concentration of free fullerene (monomer) that results in the decrease in solubility observed. Thermodynamic evidence for solute aggregation was provided by Smith et al.[5] who measured the enthalpies of solution for C_{60} in several solvents and proposed a theory for the unusual temperature dependence of the solubility that invokes the formation of a solvated solid phase.

There have been several spectroscopic studies of fullerene aggregation. Chu[6] employed light scattering methods to examine the aggregation of C_{60} in a room-temperature, benzene solution at concentrations near the solubility limit. It was found that aggregates grew exponentially with time and could be destroyed by modest mechanical agitation of the solution. Sun et al.[7] have recently demonstrated that fullerene aggregates in solution may be photopolymerized. Ahn et al.[8] reported that photoluminescence (PL) spectra of C_{60} aggregates in concentrated toluene solutions (0.7−3 mM) resembled that of the crystalline solid except that the line widths were broader and that the energy of the electronic origin of aggregate emission was located between that of the crystal and the monomer. The observed blue shift of the spectrum relative to the crystal was attributed to quantum confinement effects. It was estimated that the aggregates were ~2.4 nm in diameter, corresponding to about three C_{60} molecules, and were weakly bound. The aggregates were believed to form at ~170 K, near the liquid-to-solid transition of toluene. Aggregation of C_{60} solute is also reported to occur in CS_2 solution,[9] and osmotic pressure measurements have indicated that C_{60} forms dimers in chlorobenzene solution.[10]

Several studies of C_{70} aggregates have also been reported. Ghosh et al.[11] observed solvatochromic behavior of C_{70} in a variety of binary solvent mixtures by optical absorption, fluorescence, and light scattering techniques and concluded that stable aggregates were formed ranging in size from ~100 to ~1000 nm. Sun and Bunker[12] reported a marked change in the absorption spectrum of C_{70} that they attributed to aggregate formation in binary solutions of toluene with varying concentrations of acetonitrile.

10.1021/jp9832591 CCC: $15.00
Published on Web 11/10/1998

In the present work, we have used both static and dynamic Rayleigh scattering, as well as PL spectroscopy to examine the kinetics of aggregation as well as the structure and photophysics of C_{60} and C_{70} fullerene aggregates. Two types of aggregates have been examined: aggregates prepared by slow growth in single-solvent solutions and aggregates formed rapidly in a binary solvent mixture using a weak and a strong fullerene solvent. In both cases, the aggregation process is distinguished from precipitate formation in that aggregation leads to a stable suspension of particles with a structure different from that of the bulk crystal, and in many cases, the aggregates carry a characteristic charge.

Experimental Section

Sample Preparation. Solutions containing fullerene aggregates were prepared by two procedures. (1) Solutions of C_{60} (1.4 mM) in benzene were prepared using spectrochemical grade benzene and C_{60} (99% purity) purchased from SES Research. The solutions were filtered through a 0.2 μm PTFE syringe filter after being stirred for at least 8 h. These solutions were studied by light scattering and PL spectroscopies and exhibited slow aggregate growth over a period of days to weeks. (2) Solutions containing aggregates of C_{70} were prepared by the method first employed by Sun and Bunker.[12] Acetonitrile, a poor fullerene solvent, was rapidly added to a solution of C_{70} in toluene. Aggregates form rapidly upon mixing, and the degree of aggregate formation can be controlled by the toluene−acetonitrile volume ratio and the concentration of fullerene. Concentrations of C_{70} ranged from 0.01 to 0.1 mM. The C_{70} crystals were grown from a toluene solution in order to compare the crystal spectrum with those of the aggregates. The crystals obtained were well-formed, thin rectangular plates.

Instrumental. In benzene solution, C_{60} aggregates are quite dilute and most of the solute is present in unassociated form. In the mixed solvent systems, the situation is reversed and the solutions contain a high concentration of aggregates and relatively little unassociated fullerene. These differences require different approaches to the spectroscopic study of the solutions.

Static Rayleigh scattering measurements were performed with a modified Brice-Phoenix light scattering spectrometer. Since the relatively concentrated C_{60} solutions absorb strongly throughout the visible region of the spectrum, a low-pressure rubidium vapor lamp was used. The principal line emission of this lamp falls in a spectral region that is free of sample absorption ($\lambda_1 =$ 780 nm, $\lambda_2 =$ 795 nm). A Spectragon LP-0760-S filter was used to block the short wavelength emission of rubidium. The instrument was equipped with a Hamamatsu 928 photomultiplier with extended red sensitivity to detect the Rayleigh scattering in the near-IR, and the cell compartment was thermostated in order to maintain the solution temperature at 25 ± 1 °C. The instrument was interfaced with a Keithley data acquisition system and an electronically activated shutter so that it could be operated continuously over the period of measurement, with sample illumination only during measurement intervals.

Dynamic (quasi-elastic) Rayleigh scattering measurements were made with a Brookhaven Instruments model BI-200 goniometer and BI-2030 autocorrelator. For these measurements, a SpectraPhysics model 125 helium−neon laser was used. The 632.8 nm radiation is weakly absorbed by fullerene solutions, and care was taken to avoid heating of the solution. Solutions with concentrations of <0.1 mM and containing large aggregates were found to scatter strongly and absorb only weakly, so heating presented little difficulty. The more concentrated benzene solutions absorbed significantly and required low laser power to avoid heating effects. Histograms of aggregate sizes were computed using the nonnegatively constrained least-squares program[13] provided with the Brookhaven Instruments BI-ISDA software package. The effective aggregate diameter was determined by employing a second-order cumulant fit[14] to the scattering data.

Electronic absorption spectra of solutions containing aggregates proved difficult to obtain because of intense Rayleigh scattering. PL spectra, however, could be recorded over a range of temperatures. In general, spectra recorded below 77 K exhibited improved resolution. PL spectra were obtained from solutions containing aggregates that had been characterized by Rayleigh scattering. These solutions were cooled in a Janis 10DT cryostat with a flow of cold gas from either a liquid helium or liquid nitrogen reservoir. PL was excited using the 488 nm emission of a Coherent Innova 90 argon ion laser. The PL was collected with a large aperture spherical lens (*f*/4), filtered with a Corning 3-67 glass filter to remove scattered laser light, and dispersed with an $^1/_4$ m scanning monochromator.

Results and Discussion

Slow-Growth Aggregates in Single-Solvent Solution. Aggregate formation may be observed by monitoring the change in scattering intensity of a solution with time. The excess scattering intensity (I_{ex}) from a solution containing fullerene molecules and aggregates is defined as[15]

$$I_{ex} = I_{solution} - I_{solvent} \tag{1}$$

The excess Rayleigh ratio (R_{ex}) is the ratio of I_{ex} to the light intensity incident on a scattering volume, and it is related to the weight-average molecular mass (M_w) of the aggregates by the following equation:

$$HC/R_{ex} = \frac{1}{M_w S(\mathbf{k}r_g)} + 2A_2C \tag{2}$$

H is an instrumental constant, and C is the concentration (g/L) of the solution. A_2 is the second virial coefficient and $S(\mathbf{k}r_g)$ is the particle scattering factor for scattering vector $\mathbf{k}$ and particle radius of gyration r_g. The scattering vector is given by

$$\mathbf{k} = \frac{4\pi n}{\lambda} \sin\left(\frac{\theta}{2}\right) \tag{3}$$

where n is the refractive index of the solution, λ is the wavelength of the scattered light, and θ is the scattering angle. For small values of the product $\mathbf{k}r_g$,

$$S(\mathbf{k}r_g) = 1 - (\mathbf{k}r_g)^2/3 \approx 1 \tag{4}$$

By measurement of R_{ex} as a function of solution concentration and scattering vector $\mathbf{k}$, we are able to obtain the values of the mass and radius of gyration of the scattering particles by extrapolating the data to the following limits:

$$\lim_{C,\mathbf{k}\to 0}[HC/R_{ex}] = 1/M_w \tag{5}$$

In the present experiments, the static Rayleigh scattering was useful chiefly for studying the effect of solvent type, temperature, and other influences on the kinetics of aggregate growth.

Figure 1 illustrates the increase in Rayleigh scattering from several benzene solutions of C_{60} (1.4 mM) due to the formation and growth of aggregates over a period of approximately 6 days. The data shown in Figure 1 illustrate the differences typically

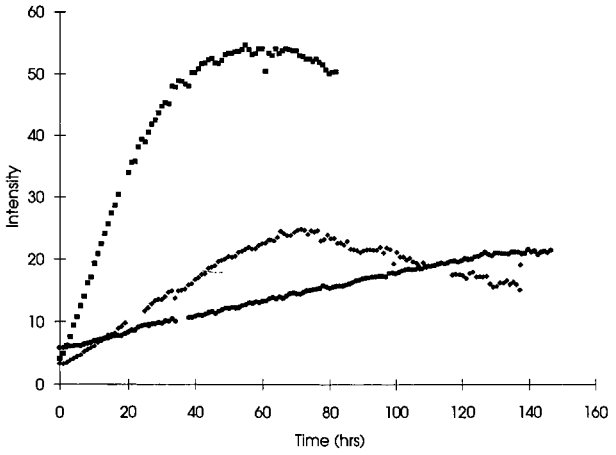

Figure 1. Time evolution of Rayleigh scattering from three nominally identical solutions of 1.4 mM C_{60} in benzene.

observed between nominally identical sample solutions in the rate of growth and the peak scattering intensity achieved. Samples with a rapid initial aggregate formation produce more or larger aggregates (stronger scattering), while slower initial growth rates are associated with the production of fewer or smaller aggregates. The differences in light scattering behavior of nominally identical solutions are plausibly due to the number of nucleation centers, which are difficult to control. In all cases, the scattering decreased at long times as large aggregates precipitated. Thus, it seems likely that the number of aggregates rather than their size is responsible for the variation in scattering.

The rate of growth of aggregates was found to depend on the surface chemistry and structure of the solution cell. When Pyrex or optical glass cells were used, a linear increase of the scattered intensity with time was always observed. Pretreatment of the cell with acid increased the rate of aggregate formation. When vitreous silica cells were used, aggregate formation was never observed, but growth could be initiated by the addition of a few small pieces of Pyrex glass to the silica cell. This behavior indicates that aggregates are nucleated at the Pyrex surface and then grow in a reaction-limited particle−aggregate manner.

We have explored factors that might contribute to the variability of the growth kinetics, including dissolved gases or impurities in the solvents and various methods of preparation of the sample solutions, all of which were found to have insignificant effects. It was discovered that the addition of a small amount of radical scavenger, 2,6-di-*tert*-butyl-4-methylphenol (BHT), to the benzene solution was effective in suppressing initial aggregate growth. This result suggested that aggregate formation might proceed via a radical-initiated mechanism. The source of the solution radicals is uncertain; however, we note that the electron−hole pairing energy for C_{60} is relatively low (~0.39 eV, in a vacuum).[16] This is the energy required for the process

$$2C_{60} \rightarrow C_{60}^{\bullet -} + C_{60}^{\bullet +} \tag{6}$$

It is likely that the energy required for this process would be substantially lower in a polar environment.

It was not possible to make accurate measurements of the aggregate mass and radius of gyration using standard static light scattering methods because the dilutions required by eq 5 might alter the aggregate mass. That is, it is not known a priori whether the aggregates are formed by a reversible process such as

$$(C_{60})_n \leftrightarrow C_{60} + (C_{60})_{n-1} \leftrightarrow ... \leftrightarrow nC_{60} \tag{7}$$

that could be displaced by dilution. In addition, it was estimated that less than 1% of the fullerene in solution was contained in aggregates so that the averaged mass of the particles from eq 5 would be heavily weighted by the unassociated solute.

Instead, aggregate dimensions and polydispersity were obtained by dynamic light scattering measurements. If the particles are monodisperse, the first-order (normalized) autocorrelation function for the scattered field, $g^{(1)}(\tau)$, is expressed by an exponential function

$$g^{(1)}(\tau) = \exp(-\Gamma\tau) \tag{8}$$

where $\Gamma = \mathbf{k}^2 D$ and D is the diffusion constant of the aggregates. A hydrodynamic radius r_h can be obtained from Stokes' law:

$$r_h = kT/(6\pi\eta_0 D) \tag{9}$$

where η_0 is the solvent viscosity. If a distribution of particle sizes is present, the autocorrelation is expressed by a distribution function. For example, the particle size distribution may be expressed by a finite number of Γ_j for the approximation

$$g^{(1)}(\tau) = \sum_j g(\Gamma_j) \exp(-\Gamma_j \tau) \tag{10}$$

The polydispersity of particle size was obtained by a fitting procedure. In benzene solutions r_h increases to ~300 nm, although total scattering begins to decrease before this size is reached because of sedimentation. The large size is not adequately reflected in the scattering intensity, indicating that very little of the fullerene is incorporated into the aggregates. Filtering, to remove the aggregates, had little effect on the absorbance of the solution, indicating that little fullerene was removed. Aggregates were stable to mechanical agitation and did not change size when diluted, indicating that aggregation is not reversible.

Aggregation in Mixed Solvents. Stable fullerene aggregates may be formed by rapid mixing of a solution of fullerene in a strong solvent with a poor fullerene solvent as first described by Sun et al. In such binary solutions, very little unassociated solute is present. Following Chu, the aggregate dimension was estimated from the static light scattering data, without dilution of the solution, in the following manner. The scattering intensity of an aggregate of mass M is given by

$$I_M(k) \approx M^2 S(\mathbf{k}r_g) F^2(\mathbf{k}) \tag{11}$$

The form factor $F(\mathbf{k}) \approx 1$ because of the small size of the primary particles. $S(\mathbf{k}r_g) \approx 1$ when $\mathbf{k}r_g \ll 1$, and $S(\mathbf{k}r_g) \approx (\mathbf{k}r_g)^{-d}$ when $\mathbf{k}r_g \gg 1$, where d is the fractal dimension of the aggregates. Thus, $I_M(k) \propto |\mathbf{k}|^{-d}$ at high $\mathbf{k}$, and d may be extracted from the limiting slope of a plot of log $I_M(\mathbf{k})$ versus log($|\mathbf{k}|$) at high k. $S(\mathbf{k}r_g)$ may be obtained with the aid of a polynomial approximation given by Lin et al.[17]

$$S(x) = (1 + C_1 x^2 + C_2 x^4 + C_3 x^6 + C_4 x^8)^{-d/8} \tag{12}$$

with $C_1 = {}^8/_3 d$, $C_2 = 3.13$, $C_3 = -2.58$, and $C_4 = 0.95$. The mass (M) of an aggregate of fractal dimension d_f is $M = m(r_g/a)^{d_f}$, where a is the molecular radius and m is the molecular mass. Substituting this relation and eq 12 into eq 11, an expression is obtained for $I_M(\mathbf{k})$ in which the aggregate dimension r_g is the only undetermined parameter. The aggregate

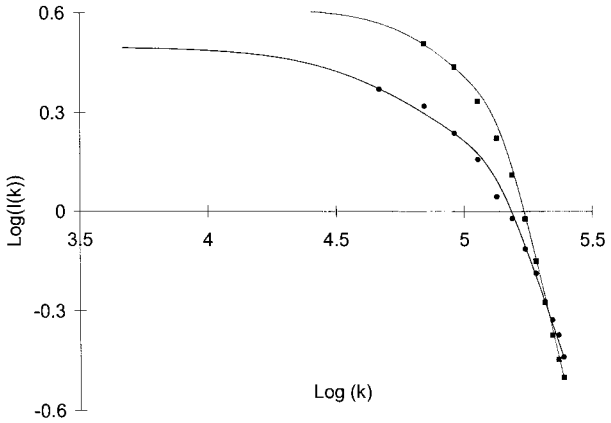

Figure 2. Plot of log $I(k)$ vs log(k). ◆ indicate data points, and the solid curve is generated by the polynomial of eq 8.

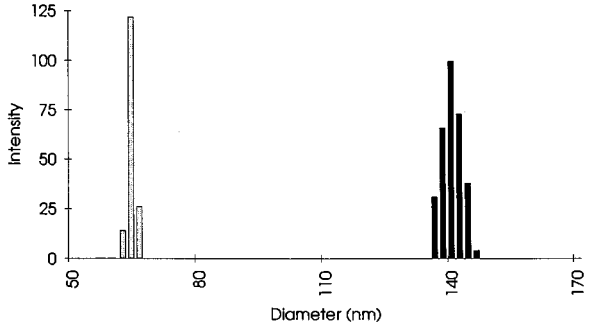

Figure 3. Histogram representation of particle size distribution in solutions containing fullerene aggregates and 65 nm polystyrene calibration spheres.

dimension may be obtained by fitting a plot of $I_M(\mathbf{k})$ versus $|\mathbf{k}|$ using r_h as the only adjustable parameter.

$I_M(k)$ was measured as a function of **k** for binary solutions (90% acetonitrile and 10% toluene by volume) containing C_{60} and C_{70} aggregates. The data are shown by the symbols in Figure 2, and the solid curves are the theoretical fits obtained using eq 11. The fractal dimension of the C_{70} aggregates was computed to be $d_f = 2.1 \pm 0.1$, and the fit shown was obtained for $r_g = 120$ nm. This fractal dimension is consistent with reaction-limited growth. For the C_{60} aggregates, the fractal dimension was computed to be $d_f = 2.9 \pm 0.1$ and the fit was obtained for $r_g = 103$ nm.

The hydrodynamic radius of the aggregates in these solutions was also determined by dynamic light scattering as described above. Figure 3 shows typical results obtained from two solutions, one containing C_{60} aggregates in an acetonitrile/toluene binary solvent solution and the other 65 ± 4 nm polystyrene spheres in aqueous solution used for calibration of the instrument. The distribution of sizes in the highly aggregated solutions (after color change) was fairly narrow and monomodal. The ratio r_g/r_h for C_{70} aggregates in the acetonitrile/toluene binary solutions was determined to be 1.0, which may be compared with the theoretical value $r_g/r_h = \sqrt{3/5} \approx 0.8$ for close-packed hard spheres.[18] The higher value obtained for C_{70} is consistent with the less densely packed structure indicated by the measured fractal dimension of 2.1. The ratio r_g/r_h for C_{60} aggregates was found to be 0.9, indicating that they are packed more densely than C_{70} aggregates, which is supported by the higher fractal dimension.

Aggregation is reversible, since the aggregates dissolve upon the addition of toluene. This can be monitored by the color change of the solution as the acetonitrile percent volume goes from 60% to 80%. Solutions that were relatively concentrated (~0.1 mM) and solutions with ~70% acetonitrile tended to produce larger aggregates and bimodal distributions. The larger aggregates (up to 800 nm) slowly precipitated and could be removed by centrifuging the solution so that the smaller (<250 nm) aggregates could be separated. The 70% acetonitrile solutions were colorless but highly scattering until centrifuged. This acetonitrile concentration lies between the predominately monomer (orange) solutions and the highly aggregated (pink) solutions. At this solvent mixture aggregates appear to incorporate most of the monomer but grow too large to remain stable in solution. We speculate that this behavior is due to a phase change occurring at high acetonitrile concentrations. The transitions from monomer solution to precipitation to stable aggregate solution are sharp and occur within a narrow range in solvent composition.

The stability of the aggregate solutions in acetonitrile/toluene binary solvent mixtures suggests that the aggregates carry a charge that stabilizes them against coalescing and, when placed in an electric field, the aggregates move rapidly to the positive electrode. It is unclear whether the charge is due to disproportionation (eq 6) or arises from the incorporation of trace impurity ions present in the polar acetonitrile solvent. The behavior of the aggregates at 70% acetonitrile indicates that disproportionation assisted by the polar medium is the cause, since the amount of impurities is not dramatically changing as one moves to 80% and is not expected to lead to the phase change behavior discussed above.

Photoluminescence Spectra of Aggregates. It was anticipated that aggregation would affect the photoluminescence of the fullerene solute. Aggregate formation may lead to the luminescence quenching via energy migration within the aggregate, or to exciton-like splittings characteristic of the crystalline material, or excimer-like fluorescence due to interactions between proximate molecules in the aggregate. To examine the effects of aggregation on the solution fluorescence spectra, aggregates solutions were prepared in binary solvent mixtures and were characterized by the techniques described in the preceding sections. The solutions were quench-cooled to form low-temperature, rigid glasses. The use of low-temperatures improved the photoluminescence quantum efficiency and the spectral resolution and stabilized the aggregates against structural changes. Repeated cycling between the room-temperature solution phase and the low-temperature glassy matrix had no effect on the photoluminescence spectrum.

The PL spectra of three solutions containing different concentrations of C_{70} aggregates are shown in Figure 4. The spectrum shown in trace a consists of single-molecule C_{70} fluorescence (15000−13000 cm^{-1}) and phosphorescence (13000−10000 cm^{-1}) and has been analyzed previously.[1,2] In traces b and c, the effect of increasing solute aggregation is manifested in the growth of a broad luminescence band with a maximum at ~13 700 cm^{-1}. The aggregate emission consists of a broad, relatively unstructured envelope, with a sharp onset at 14 700 cm^{-1} at the crystal fluorescence origin followed by a nearly exponential tail that extends into the near-infrared. Some features of the monomer PL appear superimposed on the aggregate PL spectrum, but it was noted that as the concentration of aggregates increased, the intensity of single-molecule fluorescence decreased.

Figure 5 compares the spectrum of C_{70} aggregates in a toluene/acetonitrile solution (trace a) with the spectrum of C_{70} powder (trace b) and with the spectrum of a C_{70} single crystal (trace c). The powder spectrum is modified from that of the

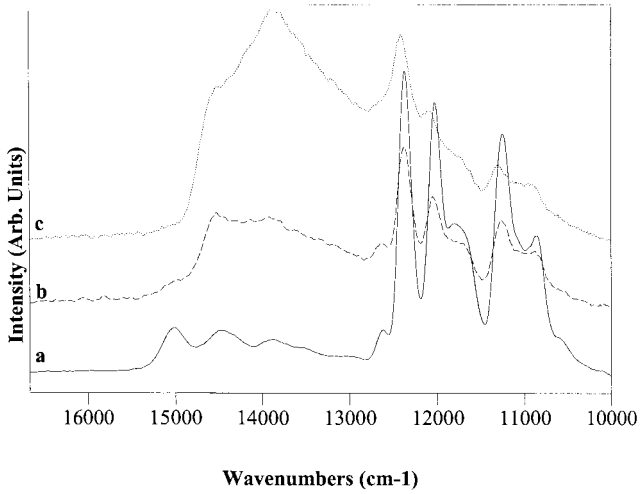

Figure 4. Photoluminescence spectra of C_{70} aggregates in toluene/acetonitrile solution: (a) few clusters; (b, c) high concentration of 200 nm diameter clusters.

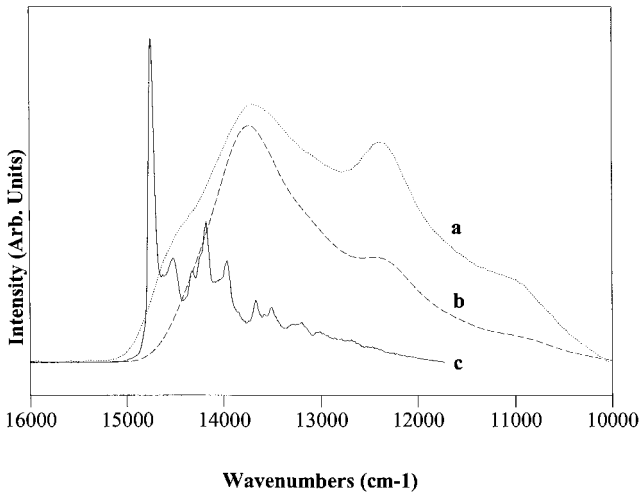

Figure 5. Comparison of the photoluminescence spectra aggregated C_{70} in (a) toluene/acetonitrile, (b) C_{70} powder, and (c) crystalline C_{70}.

crystal by the presence of many surface or defect states that contribute to the inhomogeneous line width. Clearly, the aggregate spectrum has features that correlate with both the powder and the crystal spectrum. For example, the high-energy shoulder ($\sim$14 500 cm^{-1}) evidently corresponds to the single-crystal electronic origin, and the broad central maximum ($\sim$13 800 cm^{-1}) correlates well with the maximum in powder emission. A similar correspondence is observed when the spectrum of C_{60} aggregates is compared with that of the powder and crystalline material. These correlations suggest that the aggregate has structural characteristics of both the crystal and the powder material. Plausibly, the aggregate has regions of crystalline order that give rise to the high-energy luminescence shoulder ($\sim$14 500 cm^{-1}) and regions of disorder that produce the characteristic surface-state maximum at $\sim$13 800 cm^{-1} in both C_{60} and C_{70} aggregates.

The 13 800 cm $^{-1}$ peak has been found to have a longer lifetime than the fluorescence electronic origin in both C_{60} and C_{70}.[19,20] Van den Huevel et al.[21] obtained an excitation spectrum showing that the corresponding feature in C_{60} is an electronic origin and not a vibronic origin as originally suggested.[22] Van den Huevel et al. attributed the peak to fullerene pairs, while Ichida et al.[20] attributed it to "charge separation" in the excited state. Pippenger et al.[23] assigned this peak to excimer emission. This accounts for the longer lifetime, the large red shift, and the quenching of the phosphorescence. It also allows for the broadness of the peak in C_{70}, as compared to that in C_{60}, due to the lower symmetry of C_{70}, which allows for multiple geometries of the dimer. This also explains the solidlike spectra obtained from solutions[8] that are not aggregated at room temperature. We obtained similar spectra, which are consistent with excimer emission from C_{60} and may be due to the formation of microcrystals upon cooling or by solution excimers in the frozen benzene matrix. We observed the excimer in C_{60} powder in conjunction with a t_{1u} vibronic origin as well as in a crystal grown in benzene. The aggregate spectrum is dominated by excimer emission with some contribution from two t_{1u} vibronic origins. As in C_{70} the aggregate spectrum is broader than the powder, which is consistent with the expected increase in disorder.

The excimer shifts observed for fullerenes ($\sim$1700 cm^{-1}) are considerably smaller than those observed in other aromatic species. Excimer formation typically results in a red shift of the peak emission intensity relative to that of the monomer by 5000−6000 cm^{-1}. The excimer red shift arises from two sources: a shift of the electronic origin of $\sim$3000 cm^{-1} and a large Stokes loss due to the molecular displacement in the excited state along the excimer interaction coordinate. The intermolecular interaction that contributes most to the shift of the electronic origin is the dipole−dipole interaction of the molecular transition dipole moments, which varies approximately as the inverse cube of the intermolecular separation. The roughly spherical geometry of the fullerenes results in a greater average separation of the distributed dipole−dipole interaction than is found in planar aromatic excimers, when both are in van der Waals contact.

The magnitude of the decrease was estimated by assuming that the transition dipole moment was uniformly distributed over the molecular structure. The computation was carried out for C_{60}, C_{70}, and several planar aromatic hydrocarbons for comparison. It was found that the dipolar interaction for the fullerenes was typically 25−30% of the interaction of planar aromatic hydrocarbons for comparable intermolecular separations.

Finally, the Stokes loss observed for the posited fullerene excimer is much less than those typically seen for planar aromatic molecules. The fullerene excimer line width is approximately 1000 cm^{-1}, while line widths of 4000 cm^{-1} are commonly observed for aromatic hydrocarbon excimer emission. This suggests that the displacement of the fullerene molecules leading to excimer formation is not as great as observed for planar aromatics, which is consistent with the smaller magnitude of the dipolar interaction.

Conclusion

Aggregation of C_{60} or C_{70} occurs in strong fullerene solvents at concentrations near the solubility limit over a period of days. Aggregation is irreversible and is dependent upon the surface chemistry of the container. Aggregation can be inhibited by addition of a radical scavenger, suggesting a radical-induced polymerization mechanism for aggregation. The concentration of aggregates relative to single molecules in solution is relatively low. The linear increase of the aggregate concentration with time suggests that the mechanism for aggregate growth is reaction-limited. The aggregate size distribution is polydisperse and increases until the aggregate diameter is approximately 600 nm, at which point sedimentation occurs.

Aggregates of C_{60} or C_{70} in binary mixed-solvent systems of toluene and acetonitrile form rapidly upon mixing the component

solutions and are formed reversibly. The fractal dimensions of the aggregates ($d_f = 2.1$ for C_{70} and 2.9 for C_{60}), determined by light scattering, are characteristic of growth by reaction-limited aggregation and indicate that the aggregates are less densely packed than the bulk crystal. Stable, monodisperse solutions of aggregates are formed when the acetonitrile concentration is greater than 75%. The photoluminescence spectra of solutions containing aggregated C_{60} or C_{70} exhibit a red-shifted fluorescence that is probably due to excimer formation.

References and Notes

(1) Argentine, S. M.; Francis, A. H.; Chen, C.-C.; Lieber, C. M.; Siegel, J. S. *J. Phys. Chem.* **1994**, *98*, 7350. Gallagher, S. H.; Armstrong, R. S.; Lay, P. A.; Reed, C. A. *J. Phys. Chem.* **1995**, *99*, 5817.

(2) Sibley, S. P.; Campbell, R. L.; Nguyen, Y.; Silber, H. B.; Argentine, S. M.; Francis, A. H. *Proc. Electrochem. Soc.* **1995**, *95*, 406.

(3) Ruoff, R. S.; Malhorta, R.; Huestis, D. L.; Tse, D. S.; Lorents, D. C. *Nature* **1993,** *362*, 140.

(4) Bezmelnitsin, V. N.; Eletskii, A. V.; Stepanov, E. V. *Progress in Fullerene Research, International Winter School on Electronic Properties of Novel Materials*, 2nd ed.; World Science: Singapore 1994; p 45.

(5) Smith, A. L.; Walter, E.; Korobov, M. V.; Gurvich, O. L. *J. Phys. Chem.* **1996,** *100*, 6775.

(6) Ying, Q.; Marecek, J.; Chu, B. *J. Chem. Phys.* **1994**, *101*, 2665.

(7) Sun, Y.-P.; Ma, B.; Bunker, C. E.; Liu, B. *J. Am. Chem. Soc.* **1995**, *117*, 12705.

(8) Ahn, J. S.; Suzuki, K.; Iwasa, Y.; Mitani, T. *J. Lumin.* **1997**, *72*/*74*, 464.

(9) Tomiyama, T.; Uchiyama, S.; Shinohara, H. *Chem. Phys. Lett.* **1997**, *264*, 143.

(10) Honeychuck, R. V.; Cruger, T. W.; Milliken, J. *J. Am. Chem. Soc.* **1993**, *115*, 3034.

(11) Ghosh, H. N.; Sapre, A. V.; Mittal, J. P. *J. Phys. Chem.* **1996**, *100*, 9439.

(12) Sun, Y.-P.; Bunker, C. E. *Nature* **1993**, *365*, 398.

(13) Provencher, S. W.; Hendrix, J.; De Maeyer, L.; Paulussen, N. *J. Chem. Phys.* **1978**, *69*, 4273.

(14) Koppel, D. E. *J. Chem. Phys.* **1972**, *57*, 4814.

(15) Chu, B. *Laser Light Scattering*, 2nd ed.; Academic Press: Boston, 1991.

(16) Salkola, M. I. *Phys. Rev. B* **1994**, *49*, 2665.

(17) Lin, M. Y.; Lindsay, H. M.; Weitz, D. A.; Ball, R. C.; Klein, R.; Meakin, P. *Phys. Rev. A* **1990**, *41* (4), 2005.

(18) Berry, G. C. *Encyclopedia of Polymer Science*, 2nd ed.; John Wiley and Sons: New York, 1987; Vol. 8, p 721.

(19) Ichida, M.; Sakai, M.; Yajima, T.; Nakamura, A.; Shinohara, H. *Chem. Phys. Lett.* **1997**, *271*, 27.

(20) Ichida, M.; Sakai, M.; Yajima, T.; Nakamura, A. *Prog. Cryst. Growth Charact.* **1996**, *33*, 125.

(21) van den Heuvel, D. J.; Chan, I. Y.; Groenen, E. J. J.; Matsushita, M.; Schmidt, J.; Meijer, G. *Chem. Phys. Lett.* **1995**, *233*, 284.

(22) Feldmann, J.; Guss, W.; Gobel, E. O.; Taliani, C.; Mohn, H.; Muller, W.; ter Meer,H. U. *Progress in Fullerene Research, International Winter School on Electronic Properties Novel Materials*; World Science: Singapore, 1994; p 416.

(23) Pippenger, P. M.; Averitt, R. D.; Papanyan, V. O.; Nordlander, P.; Halas, N. J. *J. Phys. Chem* **1996**, *100*, 2854.